AD

TECHNICAL NOTE TN-1163

AN ANALYSIS OF LOCAL TEMPERATURE PROFILES ENCOUNTERED IN THE ALUMINUM CARTRIDGE CASE DRILLED HOLE EXPERIMENT

by

WALTER H. SQUIRE
REED E. DONNARD

August 1971

DEPARTMENT OF THE ARMY
FRANKFORD ARSENAL
Philadelphia, Pa. 19137

54

DISPOSITION

Destroy this report when it is no longer needed. Do not return it to the originator.

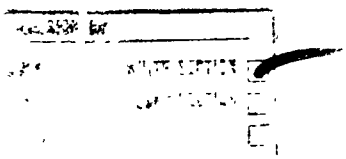

A

DISCLAIMER

The findings in this report are not to be construed as an official Department of the Army position unless so designated by other authorized documents.

TECHNICAL NOTE TN-1163

AN ANALYSIS OF LOCAL TEMPERATURE PROFILES ENCOUNTERED IN THE ALUMINUM CARTRIDGE CASE DRILLED HOLE EXPERIMENT

by

WALTER H. SQUIRE
REED E. DONNARD

AMCMS Code: 552D.11.23200.11

Ammunition Development & Engineering Laboratories
FRANKFORD ARSENAL
Philadelphia, Pa. 19137

August 1971

ABSTRACT

The consequence of propellant gas flow through a split in the cartridge case sidewall is usually more serious with aluminum cases than it is with brass cases. In order to gain a better understanding of the failure phenomenon experienced with aluminum cartridge cases, a combination experimental and theoretical program was initiated to study the failure dynamics using intentionally induced failures. This report covers only the surface temperature history of a drilled hole as a function of time and propellant gas flow. An analytical model was constructed from existing solutions to previously well investigated phenomena.

The utilization of this model predicts that the surface of a 0.0135 inch hole in an aluminum case reaches the melting point early in the internal ballistic cycle when otherwise unrestricted flow of propellant combustion gas and products through the hole are allowed to ensue.

Application of this same analysis to a brass case indicates that the melting point of the surface of a hole in the case is only approached at a point in time late in the internal ballistic cycle.

Unclassified

Security Classification

DOCUMENT CONTROL DATA - R & D

(Security classification of title, body of abstract and indexing annotation must be entered when the overall report is classified)

1. ORIGINATING ACTIVITY (Corporate author) Frankford Arsenal Philadelphia, Pa. 19137 Attn: SMUFA-K2200	2a. REPORT SECURITY CLASSIFICATION Unclassified 2b. GROUP n/a

3. REPORT TITLE

AN ANALYSIS OF LOCAL TEMPERATURE PROFILES ENCOUNTERED IN THE ALUMINUM CARTRIDGE CASE DRILLED HOLE EXPERIMENT

4. DESCRIPTIVE NOTES (Type of report and inclusive dates)

Technical research report

5. AUTHOR(S) (First name, middle initial, last name)

REED E. DONNARD
WALTER H. SQUIRE

6. REPORT DATE	7a. TOTAL NO OF PAGES	7b. NO. OF REFS
August 1971	48	16

8a. CONTRACT OR GRANT NO.	9a. ORIGINATOR'S REPORT NUMBER(S)
AMCMS Code: 552D.11.23200.11 b. PROJECT NO. c. d.	TN-1163 9b. OTHER REPORT NO(S) (Any other numbers that may be assigned this report)

10. DISTRIBUTION STATEMENT

Approved for public release; distribution unlimited.

11. SUPPLEMENTARY NOTES	12. SPONSORING MILITARY ACTIVITY
	SASA

13. ABSTRACT

The consequence of propellant gas flow through a split in the cartridge case sidewall is usually more serious with aluminum cases than it is with brass cases. In order to gain a better understanding of the failure phenomenon experienced with aluminum cases, a combination experimental and theoretical program was initiated to study the failure dynamics using intentionally induced failures. This report covers only the surface temperature history of a drilled hole as function of time and propellant gas flow. An analytical model was constructed from existing solutions to previously well investigated phenomena.

The utilization of this model predicts that the surface of a 0.0135 inch hole in an aluminum case reaches the melting point early in the internal ballistic cycle when otherwise unrestricted flow of propellant combustion gas and products through the hole are allowed to ensue.

Application of this same analysis to a brass case indicates that the melting point of the surface of a hole in the case is only approached at a point in time late in the internal ballistic cycle.

DD FORM 1 NOV 65 1473 REPLACES DD FORM 1473, 1 JAN 64, WHICH IS OBSOLETE FOR ARMY USE.

unclassified

Security Classification

14 KEY WORDS	LINK A		LINK B		LINK C	
	ROLE	WT	ROLE	WT	ROLE	WT
aluminum cartridge case						
failure dynamics						
gas dynamics						
heat conduction						
boundary layer development						

FOREWORD

The authors would like to express their appreciation to Mr. Ludwig Stiefel, Frankford Arsenal Propellant Chemistry Branch, for providing the many thermodynamic and thermochemical propellant inputs, and to Mr. Peter B. Ayyoub, Frankford Arsenal Applied Ballistics Branch, for his assistance in formulating the gas flow model.

TABLE OF CONTENTS

List of Tables

List of Figures

GLOSSARY

A	Surface area of bore
A_s	Surface area of radiating gas column
C	Initial propellant charge
C_p	Specific heat at constant pressure
C_v	Specific heat at constant volume
D	Diameter of bore
E	Constant used in Reynolds analogy
K	Stefan-Boltzmann constant
L	Length of bore
M	Local Mach number
M_i	Mach number at position i
MW	Molecular weight of propellant gases
Nu_z	Nusselt number
P	Gas pressure
P_r	Prandtl number
Q	Radiated energy
$Q_{gas \rightarrow solid}$	Total thermal energy transferred from the gas to the solid
R	Gas constant
Re_z	Reynolds number (based on length)
RF	Recovery factor
T	Gas temperature
T_{aw}	Adiabatic wall temperature
T_i	Initial temperature of solid
T_g	Characteristic gas temperature
T_s	Temperature in solid
T^*	Reference temperature
ΔT	Change in temperature due to radiation
a	Radius of bore
f	Friction factor
h_{cz}	Heat transfer coefficient
k	Thermal conductivity

GLOSSARY - Cont'd

k_g	Gas thermal conductivity
ℓ	Length dimension defined by $v_\infty (\Delta t)$
n	Number of moles of propellant gas
q	Heat flux
r	Distance in radial direction from bore's centerline
t	Time
Δt	Time interval for radiation to occur
v	Gas velocity
x	Distance into solid (cartesian variable)
z	Distance along bore's axis
δ	Boundary layer thickness
δ^*	Boundary layer displacement thickness
$\epsilon(t)$	Thickness of thermal layer
γ	Ratio of specific heats
κ	Thermal diffusivity in solid
ρ	Gas density
μ	Absolute viscosity of propellant gas

Subscripts

o	Stagnation state (Reservoir)
s	Properties characteristic of the solid
∞	Free stream condition

INTRODUCTION

The United States Army is performing exploratory development to determine the engineering parameters required for reliable use of aluminum cartridge cases in high pressure, small caliber-ammunition applications. This work is based on the need to create lightweight weapon systems in near future applications. Conservation of copper resources is an added benefit to be gained from success in this effort.

Past experience has shown that direct substitution of aluminum cased ammunition in existing weapon systems poses a potential problem with respect to the case failure mechanism.[1] In certain instances a case failure, commonly called "burn-through," results in gas-washed and eroded case surface and represents a possible damage mechanism to both weapon operator and weapon. Evidence to date suggests that this phenomenon results from a mechanical failure of the cartridge case during the internal ballistic cycle or firing of the weapon.

When a brass case fails during firing, the rifleman often is unaware that a failure has occurred. The usual consequences of such a failure are slight gas leakage at the weapon breech, discoloration of the case at the point of the defect and, possibly, a slight change in cyclic rate of the weapon when such firing is in the automatic mode. On the other hand, the firing of ammunition having a defective aluminum cartridge case can be far more spectacular. Here, there can be an efflux of very luminous gases at the weapon breech which results in weapon and case damage; the rifleman is also exposed to hazard under these circumstances.

The positive approach taken to serve as the basis for successful application of aluminum cases consists in understanding and solving the problem. Prior to initiation of the "understanding the problem" phase, various suppositions were expressed as to the mechanism of this phenomenon.[2] One technique was found to be reliable in producing the characteristic flash and metal erosion which has sometimes been observed during firing of defective aluminum cased ammunition.

---

[1] Miller, S., "Design, Development and Fabrication of 100,000 Cartridges, Ball, Caliber .50, M33 Type Assembled with Case, Cartridge Aluminum, Caliber .50, FAT 39," Technical Report R-1265, June 1956, Frankford Arsenal, Philadelphia, Pa.

[2] Summerfield, M. "Letter to Reed E. Donnard; Subject: 'Cartridge Burn-Through Problem'," Sept 1969, Princeton University, Guggenheim Aerospace Propulsion Lab., Princeton, New Jersey.

This technique consisted in preplacing a gas path in the case by drilling a hole through the extractor groove region to the interior of the case before the case was assembled into a cartridge. Thus, this intentional case defect served as an excellent means for observing this phenomenon called "burn-through" in the actual weapon/ammunition environment. For, after all, this represented the "real world" in which the problem existed and in which it had to be solved. Aluminum cased cartridges fired in this manner exhibited the characteristics normally identified as a "burn-through." Other techniques were used to study this failure mechanism but they will be discussed in another report.

An observation that propellant gas flow through a path in the case is the underlying process whereby "burn-through" is manifested was demonstrated in an experiment wherein propellant gas flow through an induced path in the case was reduced to almost nil by the use of a special weapon bolt/chamber design. There was no damage to the case or weapon test fixture even though a gas path existed in the case wall at a location where typical case and weapon damage would have otherwise been obtained. Stopping or, at least, drastically reducing propellant gas flow through the path in the case eliminated the damage.[3] Since the physical properties of aluminum and brass differ markedly (density, specific heat and melting point), the results of propellant gas flow through a path in cases made from these materials also differ significantly. Table I comparing these properties was abstracted from reference 4. In addition to these property differences, chemical activity of aluminum alloy is much greater than that of brass.

The study to identify the parameters associated with the failure mechanism of the aluminum case and to ascertain their effect on the severity of resultant system damage is, by necessity, broad in nature. Such aspects as the relationship of propellant gas flow, energy transfer from the propellant gas to exposed case surface, heating response of the exposed case surface and chemical reactivity of the aluminum case material are under investigation.

The subject matter of this report is concerned with one part or building block in the model that will evolve to describe this phenomenon. Material contained herein describes the local or surface temperature profile along the gas path (here a drilled hole) as a function of time and the energy transfer available from the combusting propellant.

[3]Unpublished data, "The Aluminum Cartridge Case 'Burn-Through' Problem-Characteristics, Isolation, and Means of Elimination," Frankford Arsenal, Pa.

[4]Lyman, T., ed., Metals Handbook, Properties and Selection of Metals, 8th ed., Vol. 1, American Society for Metals, Novelty, Ohio, 1961.

TABLE I.
Comparison of 70-30 Brass and 7075 Aluminum

Property	70-30 Brass	7075 Aluminum
Density (lb_m/ft^3)	532.52	174.80
Thermal conductivity (BTU - ft/ft^2 hr °F)	70.00	70.15
Specific heat (BTU/lb_m °F)	0.09	0.23
Thermal diffusivity (ft^2/hr)	1.46	1.74
Solidus temperature (°F)	1680	890
Liquidus temperature (°F)	1750	1180

STATEMENT OF THE PROBLEM

The mathematics developed herein describe the heat flux resulting from the fast moving propellant gases through the induced orifice and allow determination of the temperature profiles in selected regions of the cartridge case. Emphasis is placed on the gas/solid interface, the interior surface of the induced orifice. Temperatures at the interior surface of the hole are referred to as "local" temperatures. To test the accuracy of the mathematical model, the appropriate physical constants and values obtained from the experiment were substituted into the equations; temperature profiles were also determined.

Three theories have been postulated to account for the failure of the aluminum cartridge case. All of these theories are based on the heating of the case as stated below:

1. It may be possible that the failure is the result of pure melting,

2. It may be possible that the failure is the result of decreased yield strength as a result of increased temperature. Then, solid and possibly vaporized aluminum will be part of the gas stream,

3. It may be possible that chemical reactions, either occurring at the surface of the cartridge case or in close proximity to the case, are initiated. This last possibility affects the heat flux to the cartridge case.

To determine the validity of the model developed in this document, the cartridge case will be assumed to remain intact (until melting) and

that there are no chemical reactions. In the event further experimentation indicates that the cartridge case undergoes structural degradations - at a temperature lower than the melting point - the analysis contained herein will also enable identification of that critical temperature. Further assumptions are:

1. Propellant gas behaves as an ideal gas,

2. Classical heat conduction equation describes the dissipation of energy in the solid until melting,

3. The physical properties of the cartridge case material are constant during the experiment,

4. It is possible to identify an average operating pressure,

5. The gas temperature is the adiabatic flame temperature,

To reiterate, it is only the object of this study to concentrate on the temperature profile aspects of the problem.

EXPERIMENTAL

The failure dynamics were studied by inducing failures. Figure 1 shows a typical 5.56 mm cartridge case and the location where small fissures were introduced in the head regions of both aluminum alloy and brass cartridge cases. Both types of cartridge case, with the small hole present, were loaded with a charge of 27.0 grains of WC 846 propellant and fired in a test weapon. Although the size and location of this hole might have been varied, this study is addressed to the hole geometry described in Figure 1. The thermochemical and thermodynamic properties of WC 846 propellant are tabulated in Appendix A.

The results of this testing are shown in Figures 2 and 3. As seen in Figure 2, the two brass cases seem unaffected after firing. However, the two aluminum cartridge cases have noticeable damage in the head region. The unfired aluminum alloy cartridge case can be used to compare the damage after firing with its initial, drilled condition. Figure 3 shows sectioned aluminum alloy and brass cartridge cases before and after firir . As indicated in the photograph, the small fissure in the brass case undergoes only a slight alteration. On the other hand, the increase in the hole's diameter of the aluminum alloy cartridge case is rather obvious.

After initiation of the primer by the weapon's firing pin, the propellant grains burn, releasing gas and increasing the pressure. This pressure is of sufficient magnitude to force the propellant gases through any unsealed opening in the cartridge case. When this opening is in the head region of the cartridge case, the gas flow is as indicated in Figure 4.

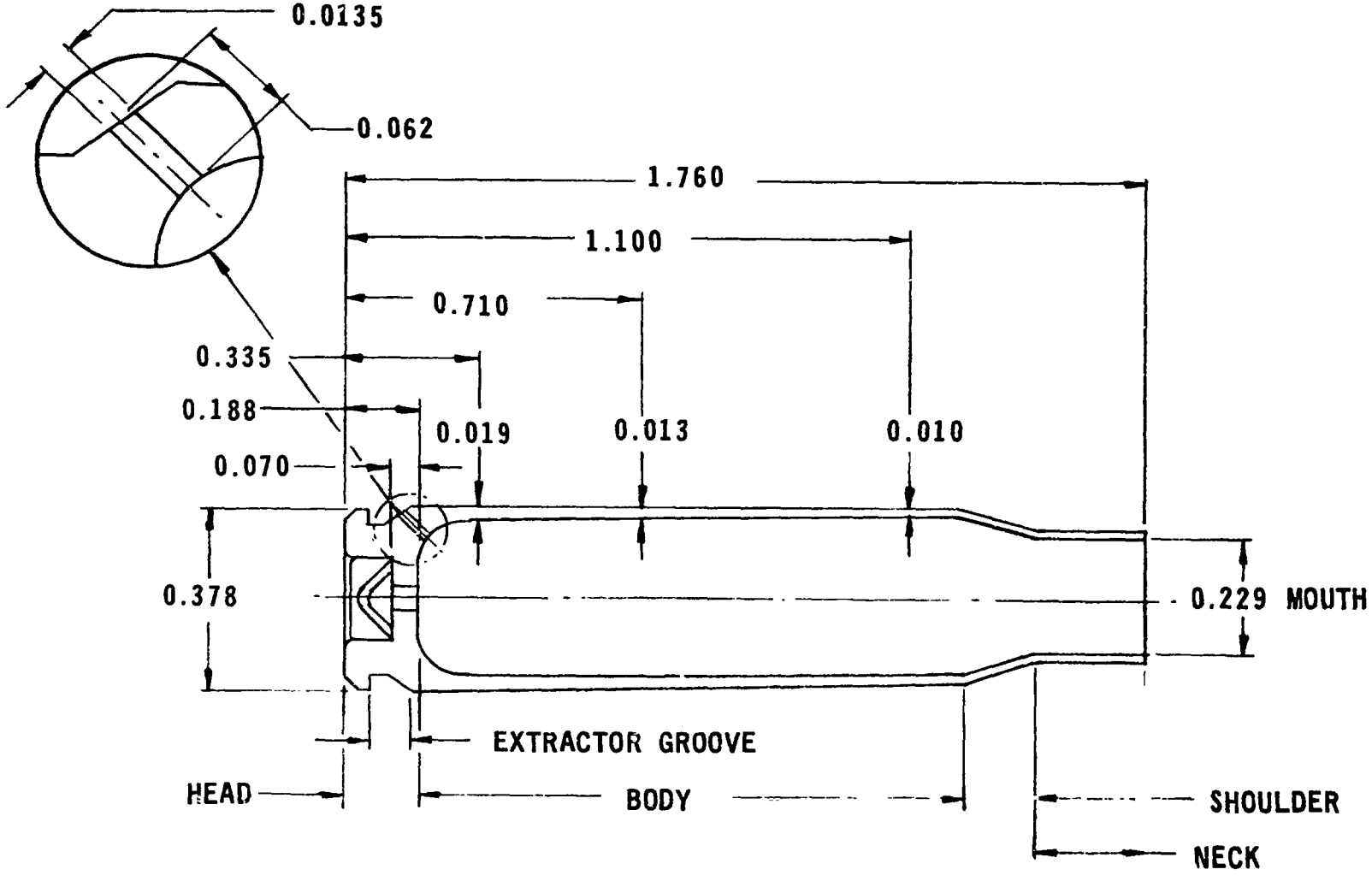

Figure 5. 5.56 mm Cartridge Case

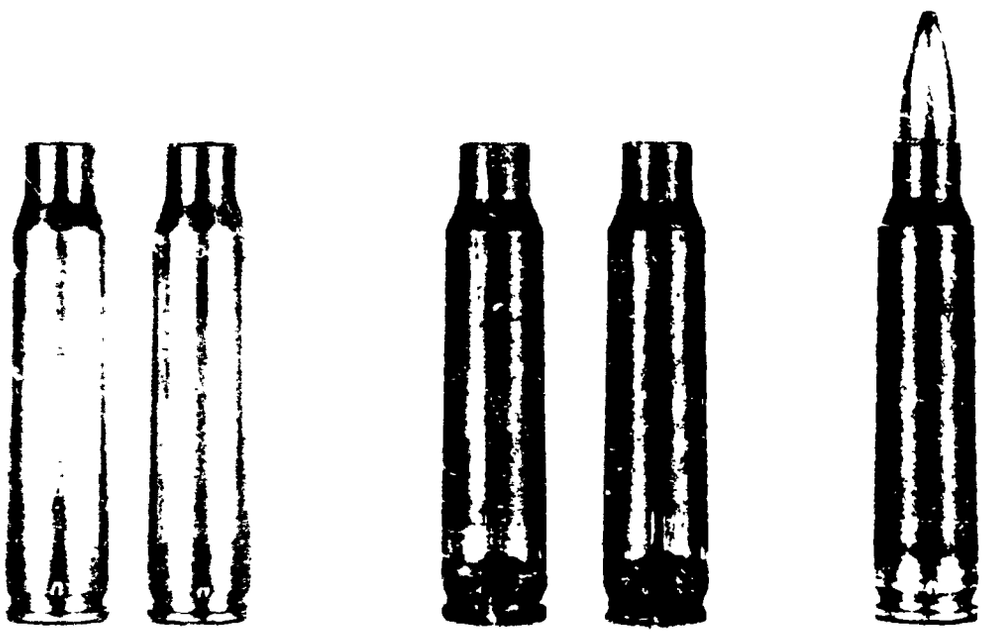

Figure 2. Drilled Hole Experiment

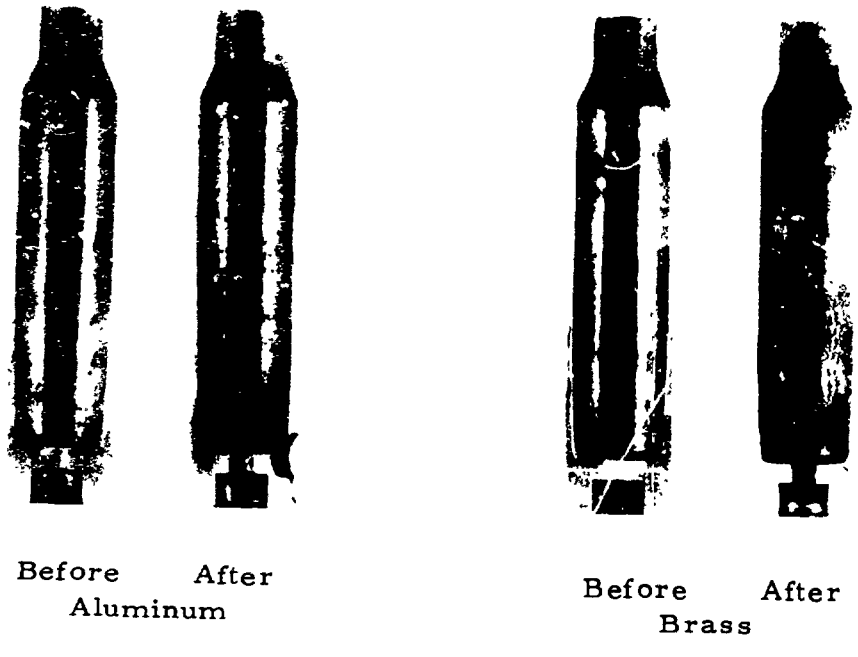

Figure 3. Sectioned Aluminum Alloy and Brass Cartridge Cases Before and After Firing

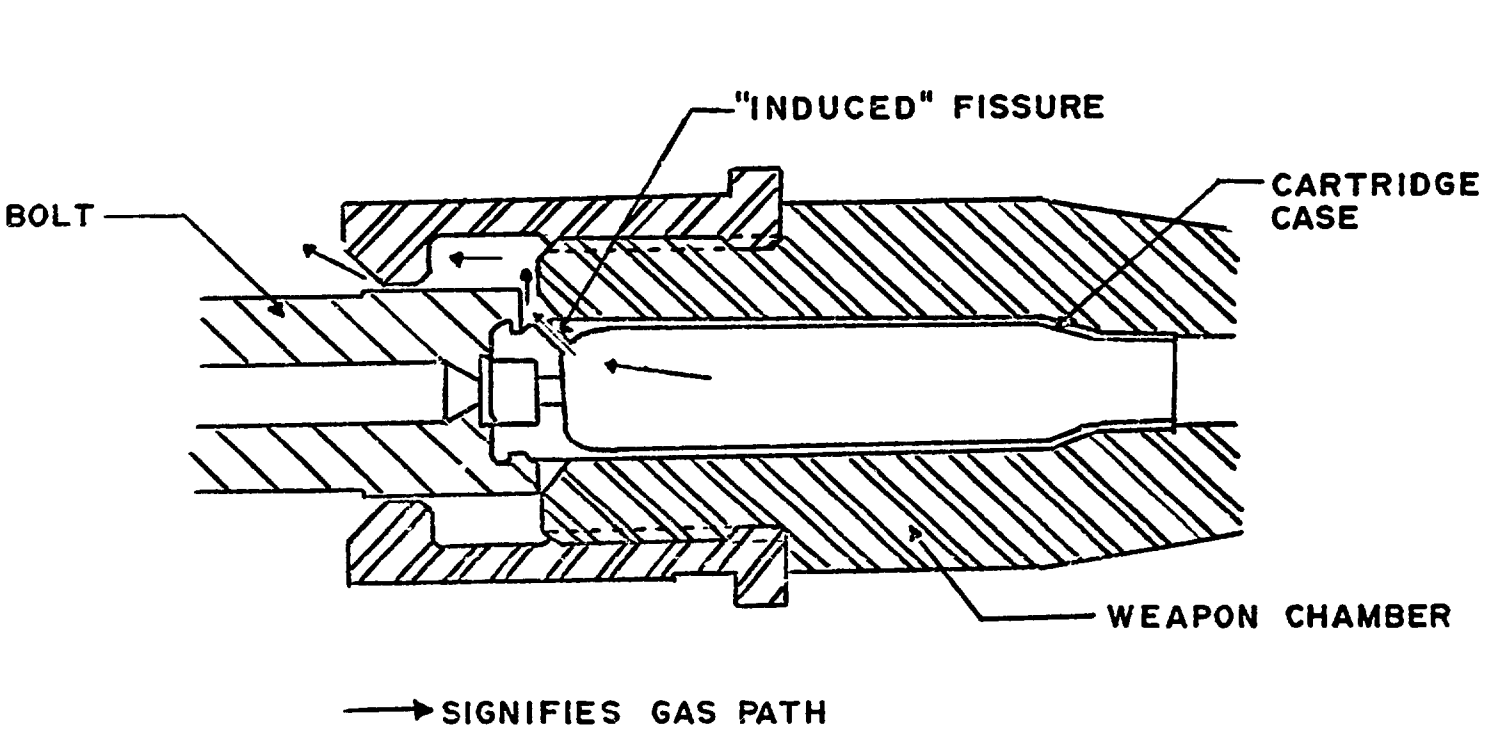

Figure 4. Schematic Representation of Problem

The generation of gas has the additional effect of expanding the sidewalls of the case until they physically touch the weapon's chamber. Although modern day weapons are designed so that the chamber offers the maximum possible support to the cartridge case, there is a small region which is totally unsupported. The existence of this region is a requirement imposed on the cartridge case by the weapon designer to allow insertion of the case into the chamber and extraction after firing. It has been observed that the erosion of case material and damage to the weapon is most severe in this region where the cartridge case is unsupported by the gun chamber. This elimination of gas flow and subsequent observation of minimal damage is borne out in the study wherein the weapon was modified to give total support to the cartridge case.[3] That is, the automatic firing mode of the weapon was sacrified by using the weapon's bolt to surround and support entirely the region of the case reserved for chambering and extraction.

To obtain pressure versus time data, a thick-walled test barrel was drilled and threaded to accept a 607A Kistler gauge. This gauge was positioned midway along the longitudinal axis of the cartridge case to measure the gas pressure. Figure 5 shows the pressure-time history of the propellant gases inside a 5.56 mm cartridge case which contained the charge of 27.0 grains of WC 846 propellant. As can readily be seen the pressure increases from 0 to 50,000 psi in approximately 0.6 milliseconds and the entire event is known to last for approximately 2.0 milliseconds.

In addition to the pressure-time curve, it was desired to monitor the duration of the gas flow from the orifice. This data was obtained by machining a test weapon to allow exposure of the head region of the cartridge case. Previous visual observation of the failure process showed the gases which exit the induced orifice in the cartridge case were luminous. Hence, positioning a photoelectric cell in the same horizontal plane and at right angles to the induced orifice provided the desired information. That is, by recording the output of the photoelectric cell on the screen of an oscilloscope it is possible to determine when the gases first exit the orifice and for how long the flow continues. A dual beam oscilloscope was used to record the pressure-time and the photoelectric cell output-time histories simultaneously. Analysis of this data indicates that gas flow begins with the first significant pressure rise and continues until the pressure curve returns to zero pressure. Hence, there is gas flowing from the orifice for a period of 2.0 milliseconds.

---

[3]Unpublished data, "The Aluminum Cartridge Case 'Burn-Through' Problem - Characteristics, Isolation, and Means of Elimination," Frankford Arsenal, Philadelphia, Penna.

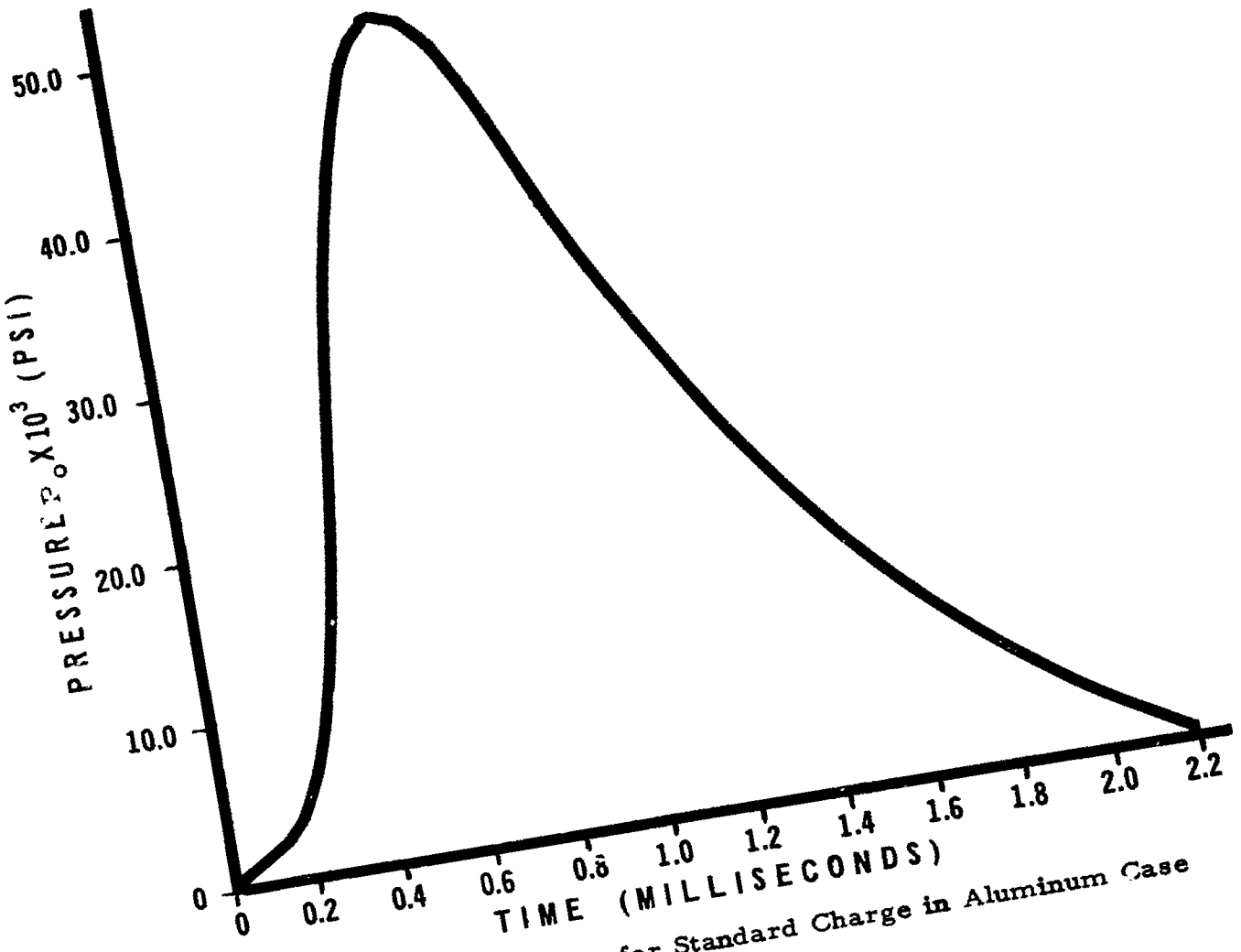

Figure 5. Pressure vs Time for Standard Charge in Aluminum Case

THEORETICAL ANALYSIS

The Flow

The approach used was to develop a mathematical model and to calculate the heat transfer rate and temperature increases at the orifice walls to determine if melting temperatures can be reached. Hence, the analysis which follows is directed to the cartridge case as shown in Figure 1. As is seen in this figure, the hole is drilled in the most massive region of the case. Also, the L/D ratio of the hole is approximately 5. Therefore, a reasonable approximation to the region of the case where the hole is drilled is that of a small hole in a medium of infinite extent in the radial direction. This description is best seen by referring to Figure 6. Distance along the axis of the bore is specified by the variable z, and distance from the center line of the bore in the radial direction is given by the variable r.

A knowledge of the propellant gas pressure and temperature, coupled with the appropriate flow theory in the bore, leads to a description of the heat flux incident on the bore's surface. The classical heat diffusion equation, written in the appropriate coordinate system, can be solved subject to boundary conditions determined from the flow analysis.

It is first necessary to describe the flow of propellant gases from the interior of the cartridge case through the induced fissure. To do so, it is important to select the most representative gas dynamic model based upon bore size. With a L/D ratio of approximately 5, the relatively small opening of 0.0135 inch in diameter, and the rapid rate of pressurization, the flow may be assumed to be choked. The additional assumption is made that the flow is developed to the point where it consists of a well defined boundary layer and a central, core region. Figure 7 is a drawing depicting this flow process. The temperature, pressure, density, and velocity as a function of position in the core region can be determined with the appropriate flow model. Determination of the nature of the boundary layer, laminar or turbulent, can be accomplished by an examination of the magnitude of the local Reynolds number.

Lee and Sears[5] suggest an adiabatic treatment of the flow be considered providing the bore is not too long (less than ten bore diameters). Admittedly, the flow process should account for the substantial transfer of energy to the bore's sidewalls since melting has been hypothesized to occur. The adiabatic assumption of the

[5]Lee, J. F., and Sears, F. W., Thermodynamics, Addison-Wesley, Cambridge, Mass., 1955.

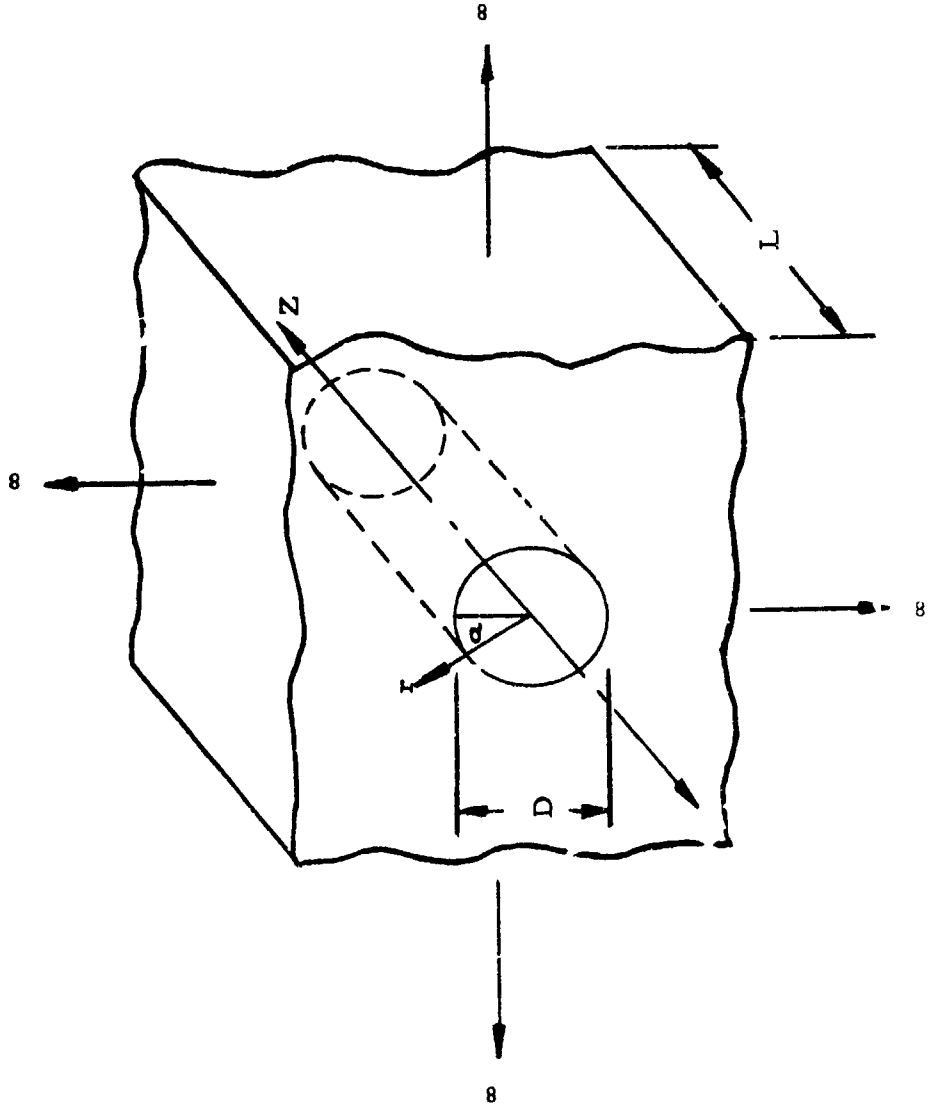

Figure 6. Two Dimensional Hole in an Intinite Medium

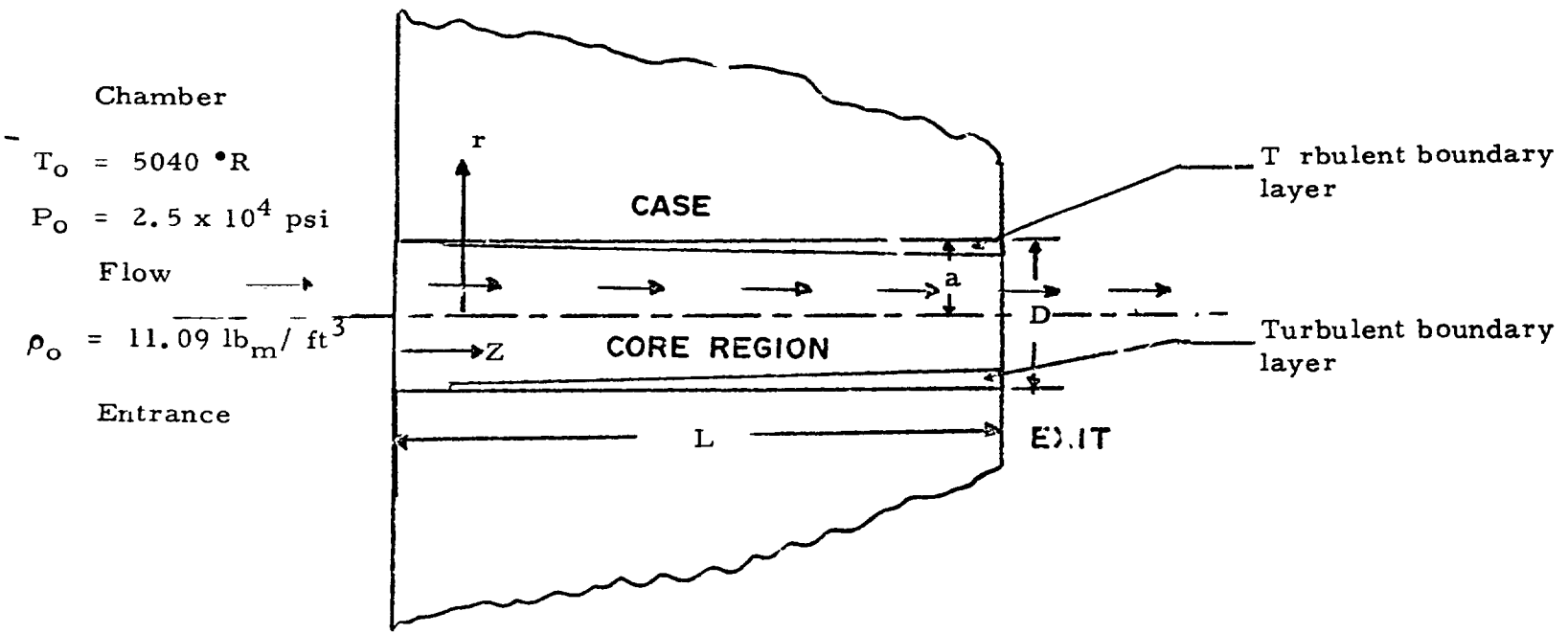

Figure 7. Schematic of Flow Process

flow does not contradict the hypothesized fact that there is substantial energy transfer. The analysis of the core region merely permits a determination of the gas conditions - i.e., temperature, pressure, density, and velocity - external to the boundary layer. It must be remembered that it is across the boundary layer that the energy is transferred to the bore's sidewalls. The gas dynamics in the core will be treated as adiabatic flow with friction in a duct of constant area.

Shapiro[6] developed a series of working formulas to describe adiabatic flow with friction in a duct of constant area. Momentum, energy, and mass equations are written for the flow of a perfect gas through an elemental control volume. Since the reservoir (chamber) conditions are available and since choking is assumed to occur at the exit, these formulas may be used to predict the temperature, pressure, velocity, and density at any position along the bore's axis. A second alternative is available. Keenan and Kaye[7] provide a series of tables for one-dimensional adiabatic flow with friction through a constant area duct. Although these tables are available for gases of differing ratio of specific heats, they are all based on an Ideal Gas Equation of State. An Ideal Gas Equation of State is used throughout this analysis to relate the intrinsic parameters of the system.

The Mach number at any position along the bore's axis is now to be determined. Lee and Sears[5] give a relationship for the bore length L, required for the flow to pass from a Mach number M_1, to a Mach number M_2 as

$$L = (L_{max})_{M_1} - (L_{max})_{M_2} .$$

Multiplication by 4f/D on both sides of the equation changes the form to

$$\frac{4fL}{D} = \frac{4f}{D} (L_{max})_{M_1} - \frac{4f}{D} (L_{max})_{M_2} \qquad (1)$$

where f is the friction factor

D is the diameter of the bore. The friction factor, f, is obtained from the Reynolds analogy

$$\frac{h_{cz}}{\rho v C_p} = E \frac{f}{2}$$

---

[5]Lee, J. F., and Sears, F. W., Thermodynamics, Addison-Wesley, Cambridge, Mass., 1955.

[6]Shapiro, A. H., The Dynamics and Thermodynamics of Compressible Fluid Flow, Vol. I, Ronald Press, New York, 1953.

[7]Keenan, J. H., and Kaye, J., Gas Tables, Wiley, New York, 1956

where h_{cz} is the film coefficient of heat transfer or simply the heat transfer coefficient

ρ is the gas density

v is the gas velocity

C_p is the specific heat at constant pressure.

With E = 1 the above equation can be rearranged to read

$$f = \frac{2\, h_{cz}}{\rho v C_p} \quad . \tag{2}$$

However, the friction factor is unknown at this time in the analysis. Shapiro[6] states friction factors in the range of 0.001 to 0.004 are realistic for the type of flow with which this analysis is concerned. Keenan and Kaye's[7] gas tables are used to determine the Mach number as a function of position along the bore for friction factors of 0.001, 0.002, and 0.004. For the time being, these three values of the friction factor will be used since h_{cz}, ρ, and v are all unknown. Later in the analysis this requirement will be relaxed and only one value will be used. The ratio of specific heats for propellant gas given in Appendix A is 1.24. Since Keenan and Kaye[7] do not provide a separate table for $\gamma = 1.24$, it is necessary to interpolate between $\gamma = 1.20$ and $\gamma = 1.30$.

With $M_2 = 1$, the ratio $(4f/D)\,(L_{max})_{M_2}$ becomes 0 and equation (1) reduces to

$$\frac{4fL}{D} = \frac{4f}{D}\,(L_{max})_{M_1} \quad .$$

Values of 4fL/D for f = 0.001, 0.002, and 0.004, L = 0.062 inch and D = 0.0135, are given in Table II. The corresponding Mach numbers for the particular friction factor are obtained from the body of the gas tables. Since the length used to calculate 4fL/D was 0.062 inch (the bore's length), these Mach numbers are the inlet Mach numbers.

Equation (1) is used again to calculate the distance required for the Mach number to change from the inlet value to some intermediate value. A typical analysis for a friction factor of f = 0.002 is given in Appendix B. Figure 8 shows the dependence of local Mach number on the position along the longitudinal axis of the bore for the three friction factors.

---

[6] Shapiro, A. H., The Dynamics and Thermodynamics of Compressible Fluid Flow, Vol. 1, Ronald Press, New York, 1953.

[7] Keenan, J. H. and Kaye, J., Gas Tables, Wiley, New York, 1956.

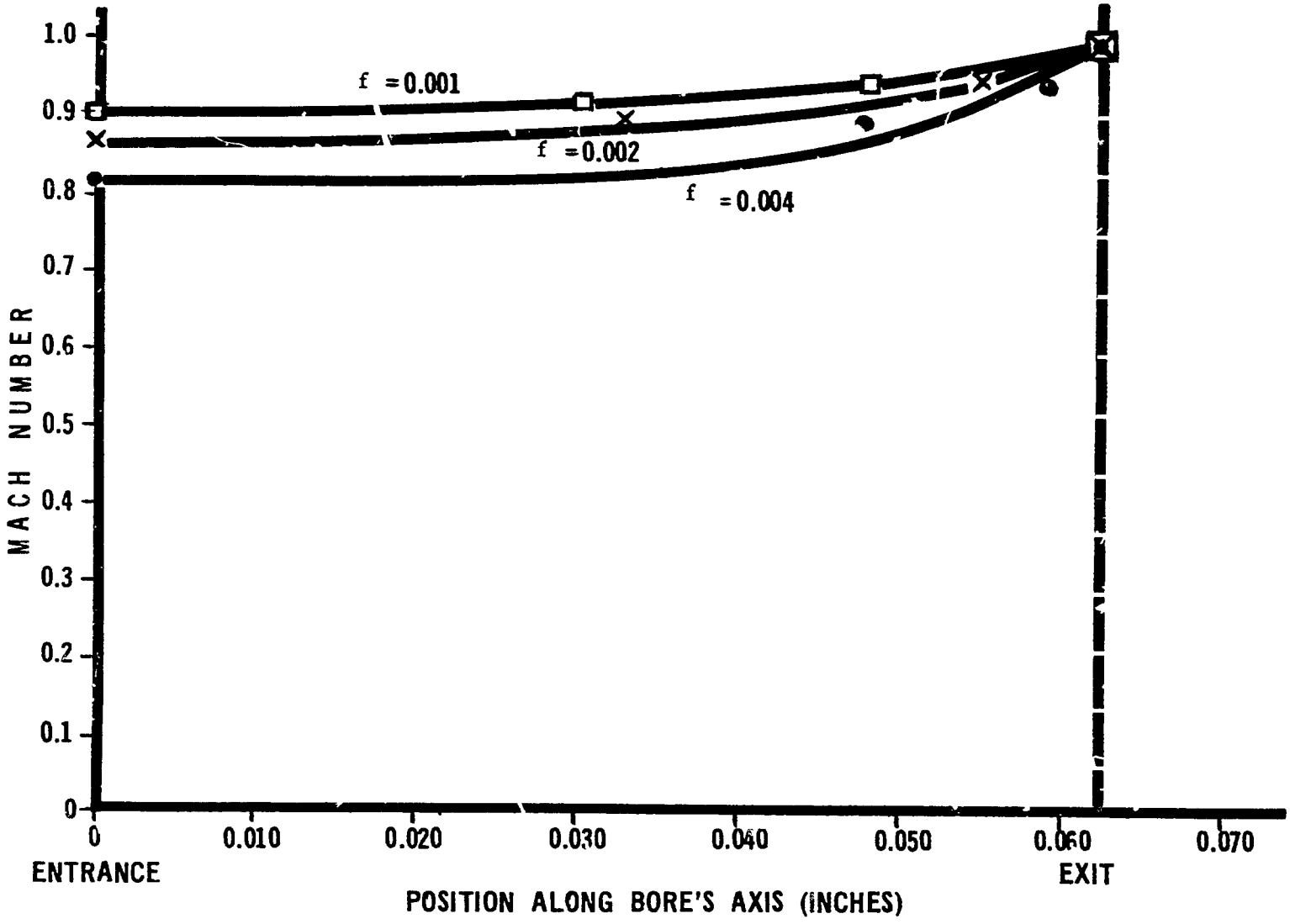

Figure 8. Mach Number as a Function of Position Along the Bore (Friction Factor as Indicated)

TABLE II.
Inlet Mach Numbers

Friction Factor	4fL/D	Mach Number
0.001	0.0183	0.900
0.002	0.0367	0.865
0.004	0.0734	0.815

Once the local Mach number is available, it is now possible to evaluate both the free stream and stagnation values for the temperature, pressure, and density at any point along the bore. The chamber conditions, as given in Appendix A, to be used throughout this analysis are:

$$T_o = 5040\ ^\circ R$$
$$P_o = 2.5 \times 10^4\ \text{psi}$$
$$R = 64.372\ \text{ft-lb}_f/\text{lb}_m\,^\circ R$$
$$\gamma = 1.24 \quad .$$

The subscript o refers to a stagnation state. With an Ideal Gas Equation of State, the gas density in the chamber (stagnation state) is given by

$$\rho_o = \frac{P_o}{R\,T_o} = 11.09\ \frac{\text{lb}_m}{\text{ft}^3} \quad . \tag{3}$$

Isentropic conditions are thought to be valid at the inlet of the bore. The isentropic conditions merely account for the flow of propellant gas from the chamber to the beginning of the bore - the inlet. For the isentropic flow, Shapiro[6] provides the following governing equations:

$$T_\infty = \frac{T_o}{1 + \frac{\gamma-1}{2} M^2} \tag{4}$$

$$P_\infty = \frac{P_o}{\left(1 + \frac{\gamma-1}{2} M^2\right)^{\gamma/\gamma-1}} \tag{5}$$

[6]Shapiro, A. H., The Dynamics and Thermodynamics of Compressible Fluid Flow, Vol. 1, Ronald Press, New York, 1953.

$$p_\infty = \frac{p_o}{\left(1 + \frac{\gamma - 1}{2} M^2\right)^{1/\gamma - 1}} \quad . \tag{6}$$

Free stream conditions are identified with the subscript ∞. The local value for the gas velocity may also be determined from the formula

$$v = M \sqrt{\gamma R T_\infty} \quad . \tag{7}$$

Using equations (4), (5), (6), and (7), with T_o, P_o, and ρ_o as previously specified and the inlet Mach number obtained from Figure 8, it is possible to specify completely all the conditions at the inlet of the bore. This information is presented in Table III.

TABLE III.
Gas Properties at the Inlet Assuming Isentropic Process

Friction Factor (-)	Mach Number (-)	Stagnation Temperature (°k)	Stagnation Pressure (psi)	Stagnation Density (lb_m/ft^3)	Free Stream Temperature (°R)	Free Stream Pressure (psi)	Free Stream Density (lb_m/ft^3)	Gas Velocity (ft/sec)
0.001	0.90	5.040×10^3	2.5×10^4	11.09	4.593×10^3	1.524×10^4	7.42	3.095×10^3
0.002	0.865	5.040×10^3	2.5×10^4	11.09	4.624×10^3	1.602×10^4	7.75	2.981×10^3
0.004	0.815	5.040×10^3	2.5×10^4	11.09	4.667×10^3	1.677×10^4	8.04	2.822×10^3

Attention is now turned to the value of the parameters, identified in Table III, at various locations in the bore. Characteristic of the adiabatic flow is the fact that the stagnation temperature remains constant throughout the bore. Equations (4), (5), (6), and (7) and the gas tables are used to determine the gas properties at the intermediate locations. These calculations are performed for a friction factor of 0.002 at positions where the Mach numbers are 0.90, 0.95 and 1.00 and are given in Appendix C. This data is shown in Figure 9.

At this point in the analysis, an approximation is used. Basically, the problem which is being studied is that of flow and heat transfer in a small bore. Kreith[8] states that for very short tubes or rectangular ducts with initially uniform velocity and temperature distribution, the flow conditions along the wall approximate those along a flat plate.

[8]Kreith, F., Principles of Heat Transfer, International Textbook Company, Scranton, Penna., 1963.

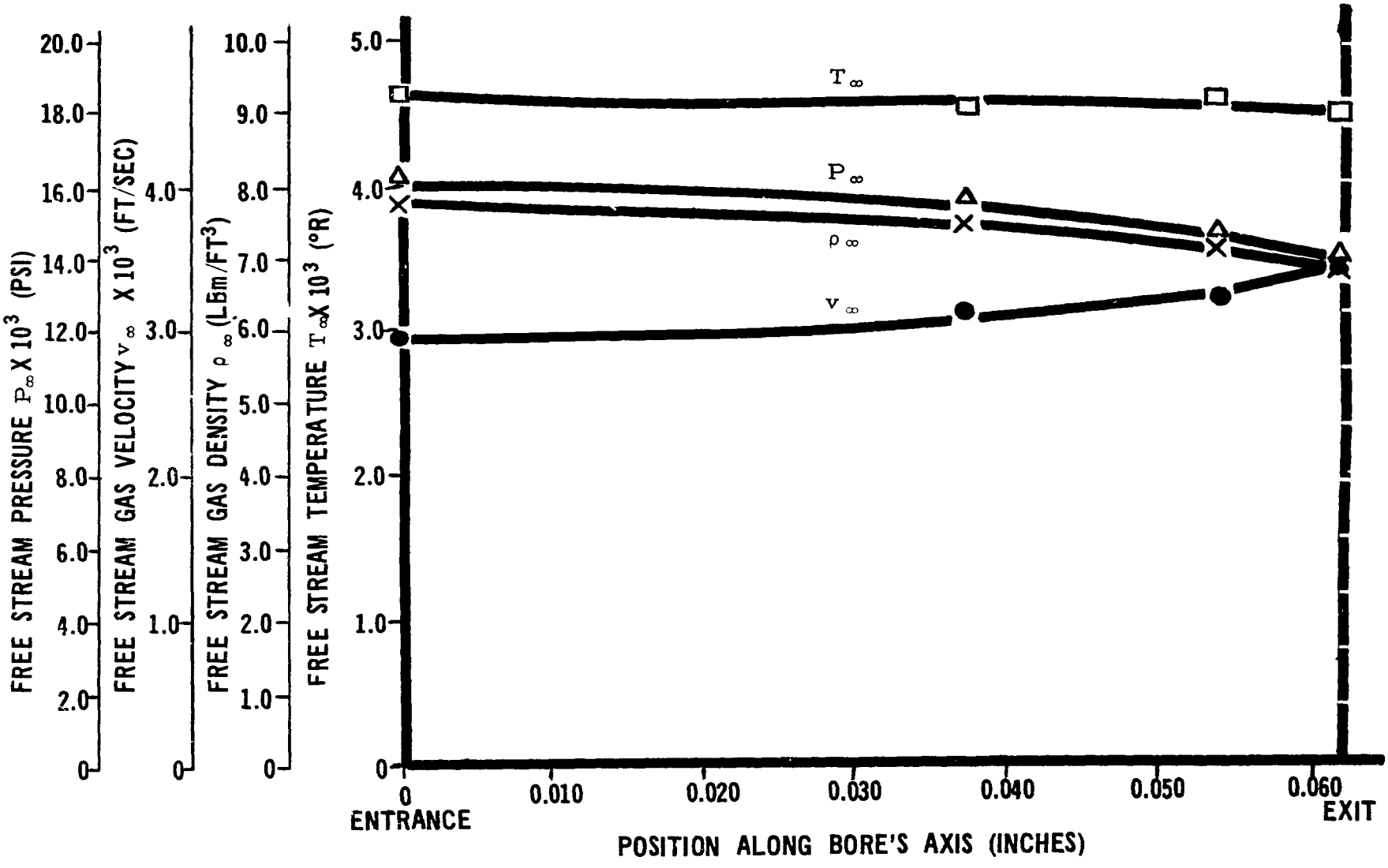

Figure 9. Free Stream Conditions vs Position Along Bore's Axis (f = 0.002)

Hence, the original two dimensional cylindrical geometry (r, z) can be replaced with a two dimensional cartesian system (x, z). Further justification for the flat plate treatment of the problem may be obtained by showing that the boundary layer displacement thickness is small compared to the bore's radius. This fact implies that the boundary layer is essentially localized near the surface of the bore.

Since the gas properties have been determined (Figure 9), it is possible to evaluate the Prandtl and Reynolds numbers. The values for the specific heat at constant pressure, absolute viscosity, and thermal conductivity are available in Appendix A. The Prandtl number, defined by $P_r = C_p\mu/k_g$ has a value of 2.905. To determine the nature of the boundary layer, turbulent or laminar, the local Reynolds number is needed. The Reynolds number, based on length, is given by $Re_z = v\rho z/\mu$. The values of the velocity, v, and the gas density, ρ, for a particular value of z are obtained from Figure 9. For example, at z = 0.031 inch (the bore's midpoint) the local Reynolds number is 1.26×10^6; likewise at z = 0.062 inch (the bore's exit) the local Reynolds number is 2.40×10^6. Kreith[8] reports that the flow over a flat plate is turbulent where the local Reynolds number is approximately 3×10^5. Comparing 3×10^5 with the calculated values of 1.26×10^6 (z = 0.031 inch) and 2.40×10^6 (z = 0.062 inch), it is possible to conclude that the flow is indeed turbulent.

It is now possible to calculate the boundary layer thickness at any point along the axis of the bore. Rohsenow and Choi[9] report that the boundary layer thickness for turbulent flow is given by

$$\delta = \frac{0.37z}{(Re_z)^{1/5}} \quad . \tag{8}$$

For the flat plate assumption to be valid it is necessary to show that

$$\frac{\delta^*}{a} << 1 \tag{9}$$

where a is the bore's radius and δ^* is the boundary layer displacement thickness. At z = 0.031 inch, the local Reynolds number, Re_z, is 1.26×10^6. Olson[10] states that the boundary layer displacement thickness for turbulent flow is given by $\delta/8$; hence, equations (8) and (9) may be combined to read

---

[8]Kreith, F., Principles of Heat Transfer, International Textbook Company, Scranton, Penna., 1963.

[9]Rohsenow, W. M., and Choi, H., Heat, Mass, and Momentum Transfer, Prentice-Hall, Englewood Cliffs, N. J., 1961.

[10]Olson, R. M., Essentials of Engineering Fluid Mechanics, International Textbook Company, Scranton, Penna., 1962.

$$\delta^* = \frac{0.37\, z}{8\, a\, (Re_z)^{1/5}} \quad . \tag{10}$$

Evaluating equation (10) at z = 0.031 inch and a = 0.00675 inch, the following result is obtained: $\delta^*/a = 0.0128$. Since δ^*/a has been determined to be 0.0128, which is very much less than one, the flat plate treatment of the bore's surface is justified.

A great deal of attention has been given to the flow characteristics of the propellant gases in the small bore. This is attributable to the fact that the flow has been identified as being the means whereby the energy is transferred to the bore's sidewalls. This energy transport can take place by basically two means, forced convection and radiation. It is therefore important to determine the Nusselt number (the dimensionless quantity relating heat transfer and fluid flow) in terms of the Prandtl and Reynolds numbers. With turbulent flow over a flat plate, Olson[10] states that a reasonable value for the Nusselt number may be obtained from

$$Nu_z = 0.0288\, (P_r)^{1/3}\, (Re_z)^{4/5} \tag{11}$$

where Nu_z implies that the Nusselt number is a function of position along the bore's longitudinal axis.

With both the Prandtl and Reynolds numbers known at this time and with the classical definition of the Nusselt number as

$$Nu_z = \frac{h_{cz}\, z}{k_g} \tag{12}$$

where h_{cz} is the heat transfer coefficient

k_g is the thermal conductivity of the propellant gas

it is possible to check on the internal consistency of the friction factor, f. Substitution of equation (11) into equation (12) and rearrangement permits identification of h_{cz} in terms of known quantities

$$h_{cz} = \frac{k_g}{z}\, (0.0288)\, (P_r)^{1/3}\, (Re_z)^{4/5} \quad .$$

Equation (2) now reads

$$f = \frac{(2)\, (0.0288)\, (P_r)^{1/3}\, (Re_z)^{4/5}\, k_g}{\rho\, C_p\, v\, z} \quad . \tag{13}$$

[10] Olson, R. M., Essentials of Engineering Fluid Mechanics, International Textbook Company, Scranton, Penna., 1962.

Evaluating equation (13) at the bore's midpoint, z = 0.031 inch, and obtaining the required values from Figure 9 and Appendix A a realistic friction factor is found to be f = 0.002.

A review of the analysis thus far is given. This section has addressed to the adiabatic flow of a perfect gas through a small bore choked at the exit plane. A characteristic design length equation was used to calculate the Mach number at any position along the bore's axis. To determine values for the gas properties at the inlet, an isentropic flow process was used. Knowledge of the local Mach number and the inlet conditions, assuming adiabatic flow through a duct of constant area with friction, allowed determination of the gas properties at any point along the bore's axis. Next, examination of the local Reynolds number identified the flow as being turbulent. Finally, a flat plate treatment of the bore's surface was justified and the appropriate Nusselt number constructed.

The Heat Transfer

As identified in the previous section, the energy transport to the bore's sidewalls is accomplished by forced convection and radiation. The heat which is transferred within the solid is governed by conduction and will be treated later in the analysis. Since the propellant gases are at a relatively high temperature, 2800°K, the effect of energy transfer due to radiation cannot be disregarded without some justification. Therefore, let us calculate the radiation heat loss with the assumption that the gas radiates like a black body under the worst possible conditions. Namely, the temperature of the gas as it flows throughout the bore is the adiabatic flame temperature, and all the propellant gas generated in the reaction flows through the induced hole. (A closed bomb experiment wherein the gas is allowed to flow through a hole 0.0135 inch in diameter for 2.0 milliseconds.)

From Appendix A, the propellant properties required for this calculation are:

Adiabatic flame temperature, $T_o = 5040\,°R$

Moles of gas produced, $n = 0.0423 \dfrac{\text{gram - moles}}{\text{gram of propellant}}$

Specific heat at constant volume, $C_v = 0.344\ \text{BTU}/\text{lb}_m\,°R$

Initial propellant charge, $C = 27$ grains

Molecular weight of propellant gas, $MW = 23.62$.

In general, with the black body assumption, the radiated energy, Q, is

$$Q = K T_o^4 (\Delta t) A_s \qquad (14)$$

where K is Stefan-Boltzmann constant $\left(0.173 \times 10^{-8} \frac{\text{BTU}}{\text{ft}^2 - \text{hr}\,(^\circ\text{R})^4}\right)$

Δt is time interval for radiation to occur

A_s is surface area of radiating gas column.

The surface area of the radiating gas column may be calculated as $A_s = 2\pi a \ell$ with ℓ a length dimension, is defined as $\ell = v_\infty (\Delta t)$ and where v_∞ is the greatest value for the gas velocity. The value for v_∞ is obtained from Figure 9 and is $v_\infty = 3400$ ft/sec. Therefore, the surface area of the radiating gas column is $A_s = 2.4 \times 10^{-2}$ ft^2. Substituting this value into equation (14), the radiated energy is $Q = 202.95 \times 10^{-4}$ BTU.

The radiated energy transferred from the propellant gas may be set equal to the internal energy change of the gas, or $Q = n C_v \Delta T$ where ΔT is the change in temperature as a result of radiation. Since the combustion of 27.0 grains of WC 846 ball propellant produces 0.0738 moles of gas, the weight of this amount of gas is given as (moles of gas) x (molecular weight) x (0.0022 pounds/gram) or 0.0038 pounds. The change in temperature can now be calculated as

$$\Delta T = \frac{Q}{n C_v}$$

$$\Delta T = 15.49\ ^\circ\text{F} \quad .$$

Hence, the temperature change in the gas as a result of radiation under the worst possible set of conditions is only 15.49°F. It is therefore concluded that the effect of radiation is insignificant.

The heating-up of the bore surface is accomplished for the most part by forced convection across a turbulent boundary layer. Assuming that the heating-up varies only along the axis of the bore, it is possible to write in general terms that

$$Q_{\text{gas}\rightarrow\text{solid}} = - A\, h_{cz} (T_s - T_g) \qquad (15)$$

where $Q_{\text{gas}\rightarrow\text{solid}}$ is the total thermal energy transferred from the gas to the solid

A is the area of the bore's surface

h_{cz} is the local heat transfer coefficient

T_s is the temperature in the solid

T_g is the characteristic gas temperature .

Olson[10] points out that the parameter h_{cz} is extremely sensitive and depends on the gas property values, such as the specific heat, thermal conductivity, viscosity, and density; the fluid flow characteristics, such as the pressure gradient and whether the flow is laminar or turbulent; and the geometry of the system. Hence, of primary interest is the determination or prediction of the magnitude of the local heat transfer coefficient, h_{cz}, or its dimensionless equivalent, the Nusselt number $h_{cz}\, z/k_g$.

Since it is more meaningful to specify a heat flux, let us rearrange equation (15) to the form

$$\frac{Q_{gas \rightarrow solid}}{A} = q = - h_{cz} (T_s - T_g) . \tag{16}$$

Substitution of equation (12) into equation (16) yields

$$q = - \frac{Nu_z\, k_g}{z} (T_s - T_g)$$

which can be transformed into a more useful form by equation (11) to read

$$q = \frac{-0.0288 (P_r)^{1/3} (Re_z)^{4/5} k_g}{z} (T_s - T_g) . \tag{17}$$

The characteristic gas temperature, T_g, is a troublesome parameter and deserves some special consideration. Rohsenow and Choi[9] point out that heat transfer driving function for high speed flow is not the free stream or stagnation temperature, but the adiabatic wall temperature, T_{aw}. Even though the velocity at the wall (surface of the plate) is zero, the adiabatic wall temperature, T_{aw}, is equivalent to the temperature which would be reached if the wall were insulated. The adiabatic wall temperature may be specified by defining a recovery factor, RF, to be

$$RF = \frac{T_{aw} - T_\infty}{T_o - T_\infty} \tag{18}$$

where as previously defined

T_∞ is free stream temperature

T_o is stagnation temperature.

---

[9]Rohsenow, W. M., and Choi, H., Heat, Mass, and Momentum Transfer, Prentice-Hall, Englewood Cliffs, N. J., 1961.

[10]Olson, R. M., Essentials of Engineering Fluid Mechanics, International Textbook Company, Scranton, Penna., 1962.

Ackerman[11] studied theoretically the turbulent boundary layer in high velocity flow over a flat rate. For ordinary high speed flow, Ackerman[11] showed that the following relationship for the recovery factor is satisfactory $RF = (P_r)^{1/3}$. However, since the flow conditions in this analysis are so drastically different than those of ordinary high speed flow some precautions are in order. The Prandtl number for the propellant gases with which this analysis is concerned is 2.905; from the above equation RF = 1.43. The fact that RF exceeds unity presents an alarming result. With RF > 1, equation (18) becomes

$$\frac{T_{aw} - T_\infty}{T_o - T_\infty} > 1$$

$$T_{aw} - T_\infty > T_o - T_\infty$$

$$T_{aw} > T_o \quad .$$

This implies that the adiabatic wall temperature can reach values above the stagnation temperature which, of course, is impossible unless chemical reactions are present. Therefore, let us set RF = 1 so that the adiabatic wall temperature is equal to the stagnation temperature. Therefore, the characteristic gas temperature, T_g, and the adiabatic wall temperature, T_{aw}, can be redefined as the stagnation temperature T_o.

Heat Transfer Within the Solid

Subject to the correct boundary conditions, conduction in the solid is governed by the Classical Heat Conduction Equation which is

$$\nabla^2 T_s = \frac{1}{\kappa} \frac{\partial T_s}{\partial t} \qquad (19)$$

where T_s is the temperature at any point, x, and at any time, t, in the solid, and κ is the thermal diffusivity = $k_s/\rho_s C_{ps}$. Since Figure 6 portrays a cylindrical geometry, one's first thought might be to cast equation (19) into cylindrical coordinates. However, it is possible to make a simplifying assumption enabling one to solve equation (19) in a semi-infinite solid subject to a boundary condition described by equation (17) with initial solid temperature, T_i.

[11] Ackerman, G., Forsch, Gebiete Ingenieurw, Vol. 13, 1942.

Ozisik[12] gives the temperature distribution in a region exterior to a cylindrical hole of radius a, extending to infinity, and subject to a constant heat flux. From his analysis it is possible to identify a phenomenological distance $\epsilon(t)$, called the thermal layer, which represents the distance beyond which the initial temperature distribution remains unaffected by the boundary condition. The results of the analysis show that the thickness of the thermal layer is given by

$$\epsilon(t) = \sqrt{6 \kappa t}$$

$$\epsilon(t)_{aluminum} = 0.20 \times 10^{-3} \text{ inch}$$

$$\epsilon(t)_{brass} = 0.18 \times 10^{-3} \text{ inch}$$

provided $a > \epsilon(t)$ and the times are relatively short. Özisik[12] further points out that for the same short times the above equation also represents the thermal thickness that would be obtained for a semi-infinite region in a cartesian system with a constant heat flux applied at $x = 0$. (Admittedly, the constant heat flux boundary condition is a different type than that described by equation (17). However, this analysis is used only to demonstrate that the thermal layer does not penetrate the solid to any significant depth.) Hence, the semi-infinite solid can be justified as a limiting case which gives results to the correct order of magnitude.

Equation (17) represents a Newton's Law of Cooling type boundary condition of the third kind. Equation (19) then reduces to

$$\frac{\partial^2 T_s(x, t)}{\partial x^2} = \frac{1}{\kappa} \frac{\partial T_s(x, t)}{\partial t}$$

subject to

$$q(0, t) = - \frac{0.0288 (P_r)^{1/3} (Re_z)^{4/5} k_g}{z} (T_s - T_g)$$

with an initial condition that $T_s(x, 0) = T_i$ and the additional boundary condition: $x \to \infty$, $T_s(x, t) \to 0$. Figure 10 portrays a graphical representation of the conduction problem.

Rohsenow and Choi[9] give a solution to such a problem and further point out that the heating of a thick body by a hot fluid at the surface approximates this case during the early stages of the transient. Their solution is as follows

---

[9] Rohsenow, W. M., and Choi, H., Heat, Mass, and Momentum Transfer, Prentice-Hall, Englewood Cliffs, N. J., 1961.

[12] Özisik, M. N., Boundary Value Problems of Heat Conduction, International Textbook Company, Scranton, Penna., 1968.

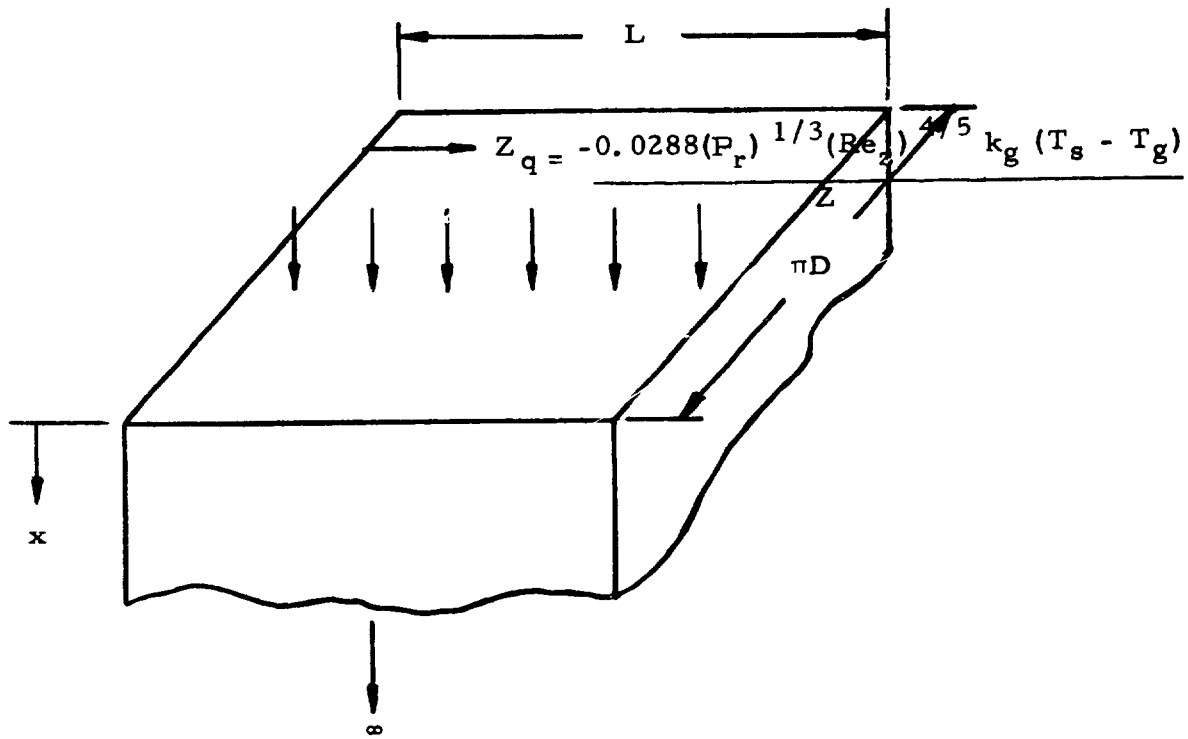

Figure 10. Flat Plate Representation

$$\frac{T_s - T_i}{T_g - T_i} = \left[\operatorname{erfc}\left(\frac{x}{2\sqrt{\kappa t}}\right) - \exp\left(\frac{x\, h_{cz}}{k_s} + \frac{\kappa t}{(k_s/h_{cz})^2}\right) \operatorname{erfc}\left(\frac{x}{2\sqrt{\kappa t}} + \frac{\sqrt{\kappa t}}{(k_s/h_{cz})}\right)\right] . \quad (20)$$

At the bore's surface (x=0), the complexity of equation (20) is reduced considerably. Although this equation has distance into the solid (x) and time (t) as the independent parameters, the position along the bore's axis (z) is hidden in h_{cz}. For this reason, the local heat transfer coefficient

$$h_{cz} = \frac{Nu_z\, k_g}{z} = \frac{0.0288\,(P_r)^{1/3}\,(Re_z)^{4/5} k_g}{z} \quad (21)$$

must be evaluated at various values of z. However, the temperature at which the fluid properties are evaluated is a reference temperature, T*, determined empirically by Eckert[13] to be

$$T^* = T_\infty + 0.50\,(T_o - T_\infty) + 0.22\,(T_{aw} - T_\infty) .$$

But since T_{aw} is set equal to T_o, the above equation becomes

$$T^* = T_\infty + 0.50\,(T_o - T_\infty) + 0.22\,(T_o - T_\infty) = T_\infty + 0.72\,(T_o - T_\infty) \quad (22)$$

Equation (22) allows determination of the reference temperature, T* ; this value is then used to evaluate the ρ_∞ and the v required by the Re_z appearing in equation (21). A typical calculation for h_{cz} at z = 0.030 inch is given in Appendix D. The general behavior of the heat transfer coefficient as a function of position along the bore's axis is given in Figure 11.

Rohsenow and Choi[9] provide a graphical solution to equation (20) in the form of a plot of dimensionless temperature, $(T_s - T_i / T_g - T_i)$, as a function of the dimensionless distance, $x/\sqrt{4\kappa t}$, for several different values of the dimensionless time, $h_{cz}\sqrt{\kappa t}/k_s$. Since this analysis is concerned only with the bore's surface (x = 0), Rohsenow and Choi's plot is reduced to the values of the dimensionless temperature along the ordinate. For this reason, it is more meaningful to plot

[9]Rohsenow, W. M., and Choi, H., Heat, Mass, and Momentum Transfer, Prentice-Hall, Englewood Cliffs, N. J., 1961.

[13]Eckert, E. R. G., Transactions of the American Society of Mechanical Engineers, Vol. 78, 1956.

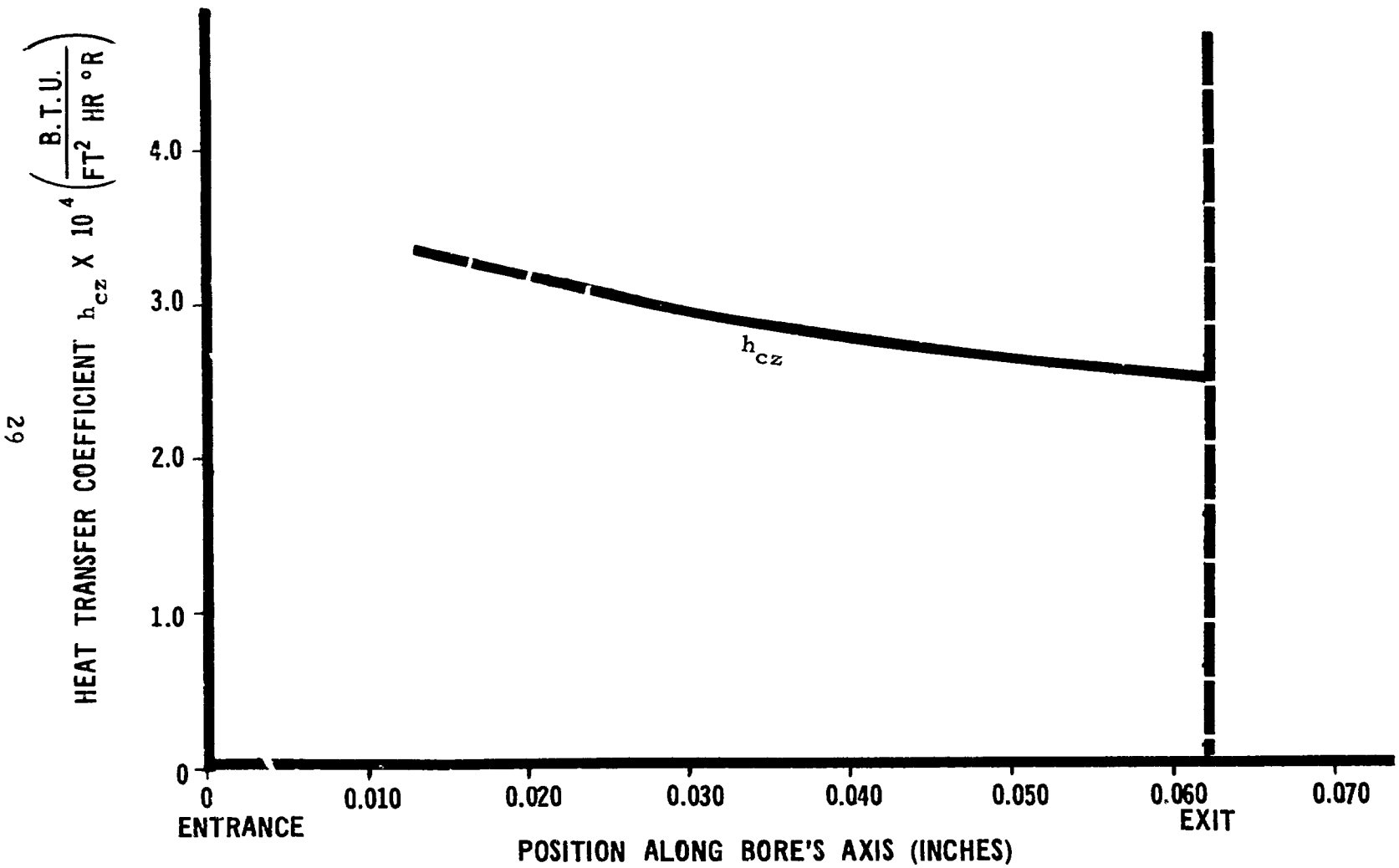

Figure 11. Heat Transfer Coefficient vs Position Along Bore's Axis

$(T_s - T_i)/T_g - T_i)$ as a function of the dimensionless time, $h_{cz}\sqrt{\kappa t}/k_s$, as is done in Figure 12. To determine the solid temperature, T_s, as a function of time at specified values of z, the stagnation temperature and the heat transfer coefficient (for that value of z) are first obtained. Both the heat transfer coefficient and stagnation temperature are assumed to be independent of the solid material. Hence, the surface temperatures as a function of time for two materials, aluminum and brass, are easily obtained by substituting the appropriate values of κ and k_s in the dimensionless parameter $h_{cz}\sqrt{\kappa t}/k_s$. Figures 13 and 14 are the bore surface temperature as a function of time for aluminum alloy 7075 and conventional 70-30 brass, for the value of z as specified.

DISCUSSION

The analytical model, developed in the preceding sections, culminating in equation (20), allows determination of the bore surface temperature given gas flow. To investigate the performance of brass and aluminum alloy cartridge cases, it is a simple matter to substitute the appropriate physical parameters - i.e., thermal conductivity and thermal diffusivity - and calculate the surface temperature as was done to prepare Figures 13 and 14. Accepting the fact that aluminum alloy 7075 melts in a range of 890 to 1180 °F whereas cartridge brass has a melting range of 1680 to 1750 °F, it is quite evident that, given gas flow for 2.0 milliseconds, the aluminum melts. The brass surface temperature, on the other hand, is lower than its melting temperature.

This analysis merely indicates that melting can contribute to failures in aluminum cartridge cases. It is well known that aluminum is a very chemically reactive metal. Hence, there exists the possibility of reaching a critical temperature at the bore's surface which initiates an exothermic reaction. This exothermic reaction can, of course, greatly alter the previously described heat flux. There is also another possibility. Small pieces of aluminum may be torn from the surface of the case and may find themselves in the highly reactive gaseous plume exiting the induced fissure. It is then possible for an exothermic reaction to occur in the gaseous atmosphere which also alters the heat flux to the surface.

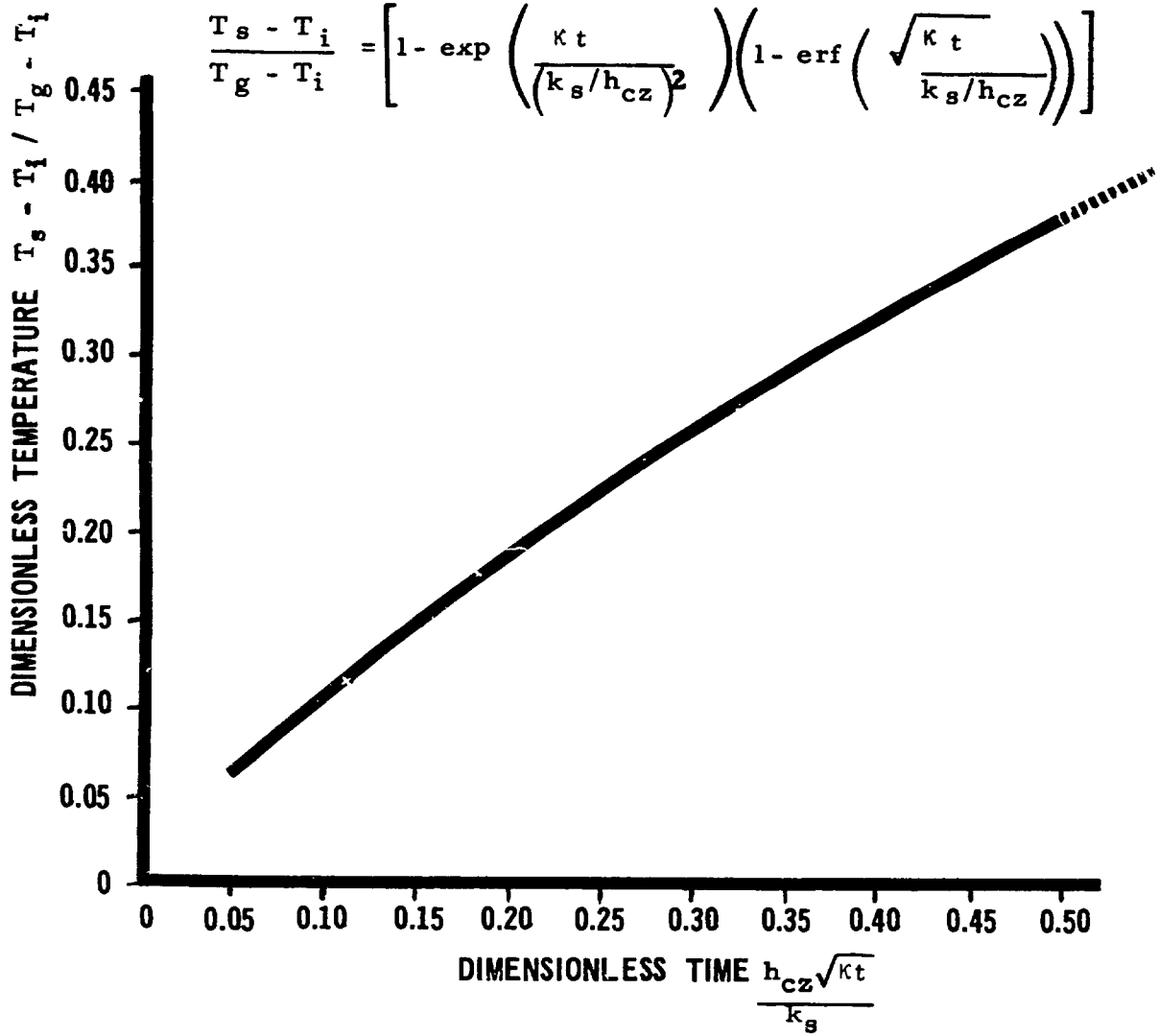

Figure 12. Dimensionless Temperature vs Dimensionless Time

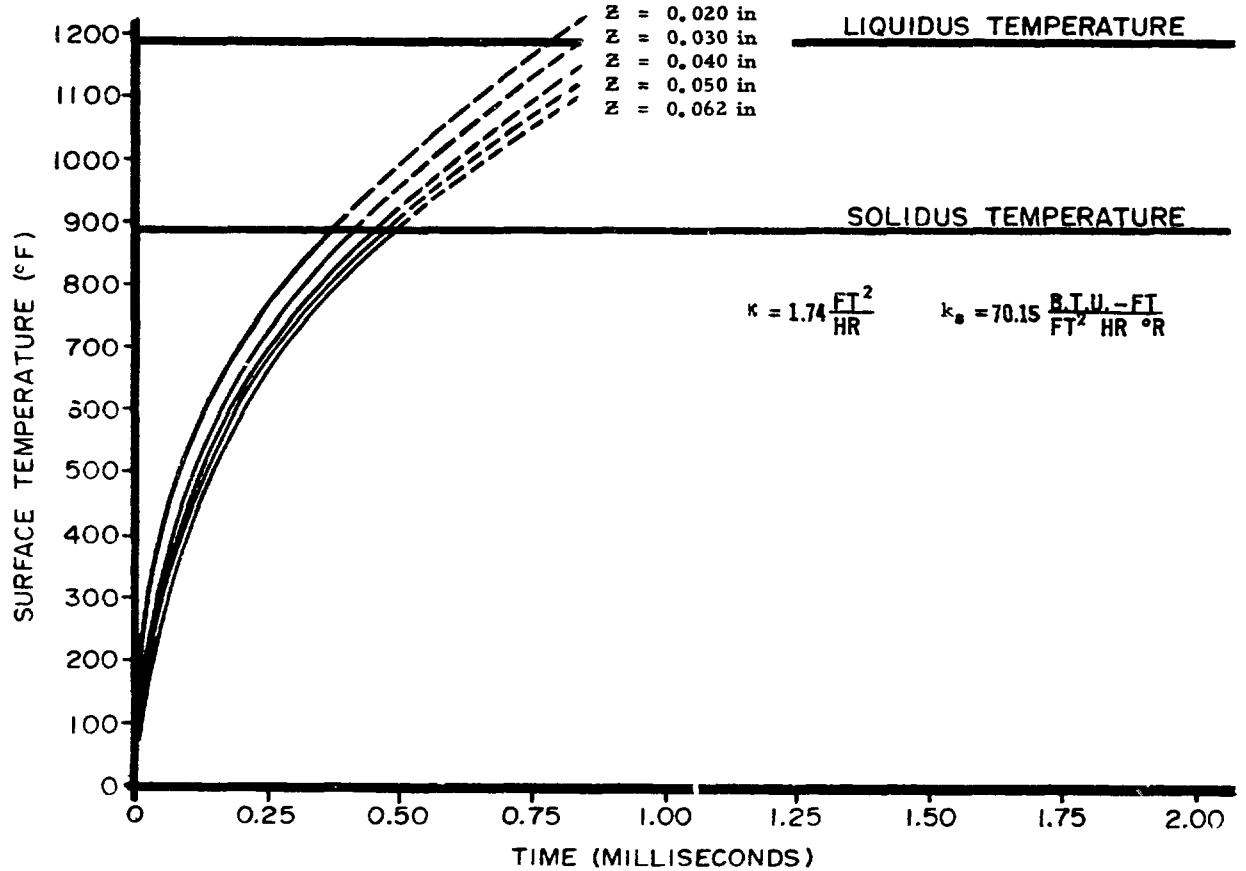

Figure 13. Temperature vs Time at Surface of Aluminum Bore (Location as Indicated)

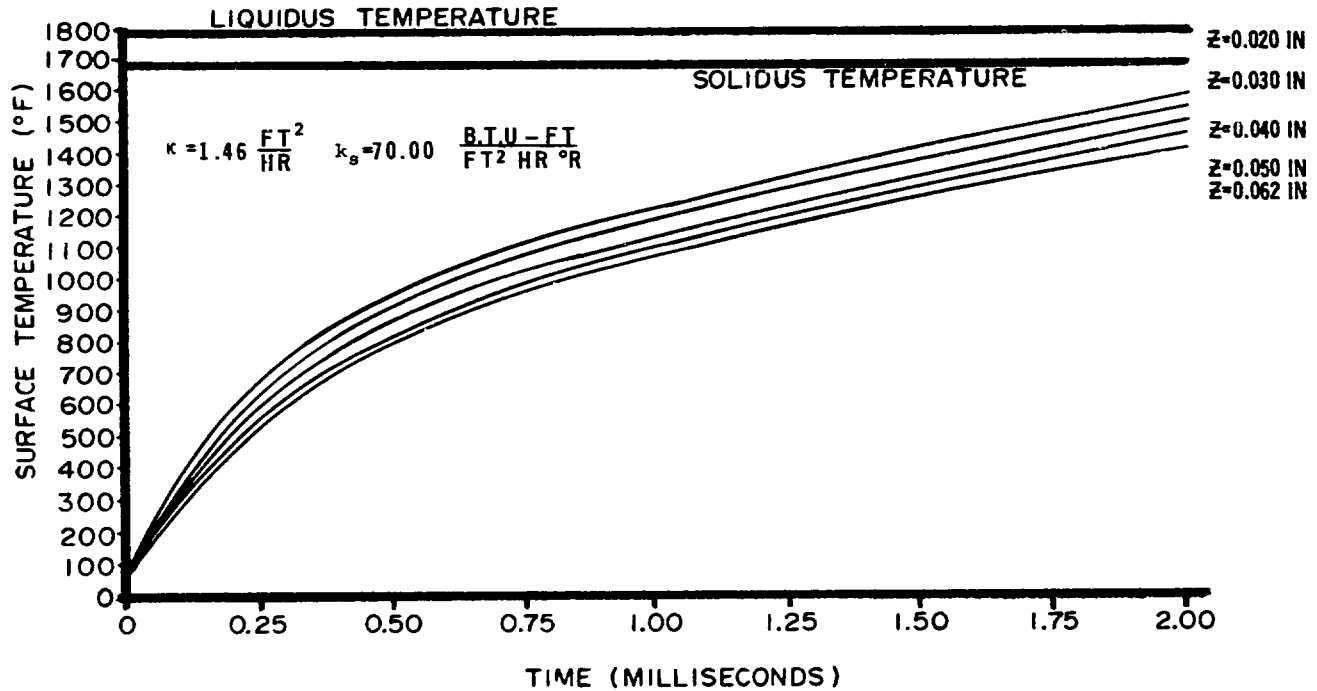

Figure 14. Temperature vs Time at Surface of Brass Bore (Location as Indicated)

CONCLUSIONS

It is concluded that:

a. Propellant gas flow through an induced path (a drilled hole) in an aluminum alloy cartridge case does increase the surface temperature in the path to the melting point when the gas path, or bore diameter, is 0.0135 inch and the internal ballistic cycle is normal for a 5.56 mm cartridge.

b. Melting of the metal in the gas path surface initiates early (approximately 0.25 milliseconds elapsed time) in the internal ballistic cycle.

c. When this analysis is applied to a brass cartridge case, under the same conditions mentioned in "a" above for the aluminum case, the melting point of gas path surface is only approached during the entire internal ballistic cycle.

RECOMMENDATIONS

It is recommended that the general analysis to construct a model that describes the nature of the aluminum case failure phenomenon be continued to include the effects of:

a. propellant gas constituency

b. case wall thickness

c. propellant temperature and pressure

d. size of the initial gas path

e. dynamics of gas path growth

f. contribution of exothermic chemistry on the heat flux

g. physical surface phenomenon of the gas path

h. additional transport phenomena-mass and momentum transfers

i. influence of shock fronts

These effects will be considered in relation to the interior ballistic cycle.

APPENDIX A

System Characteristics

I. Interior Ballistics Data
Standard Charge, C = 27.0 grains
Average Gas Pressure, $P_o = 2.5 \times 10^4$ psi

II. Propellant Composition

Ingredient	Percentage
Nitroglycerin	9.71
Dinitrotoluene	0.71
Diphenylamine	0.90
Dibutylphthalate	5.96
Nitrocellulose (13.5% N)	81.96
Moisture and volatiles	0.85
Residual solvent	0.29
Calcium carbonate	0.46
Sodium sulfate	0.07 (nominal)

III. Propellant Product Gas Properties

Adiabatic flame temperature, T_o[14] = 2800°K = 5040° R
Gas constant, R = 64.372 ft-lb_f/lb_m°R
Moles of gas produced, n[14] = 0.0423 gram-moles/gram of propellant
Specific heat at constant volume, C_v[15] = 0.344 BTU/lb_m°R
Specific heat at constant pressure, C_p = 0.427 BTU/lb_m°R
Ratio of specific heats, γ[14] = C_p/C_v = 1.24
Molecular weight, MW[16] = 23.62
Absolute viscosity, μ[15] = 4.72×10^{-5} lb_m/ft-sec

---

[14] Unpublished Data, "Smokeless Powder for Small Arms Ammunition, Nominal Characteristics of Standard Products," Olin Corporation, New Haven, Conn., Oct. 1966.

[15] Price, E. W., et al., "Theory of Ignition of Solid Propellants," AIAA Journal, Vol. 4, July 1966.

[16] Stiefel, L., and Hody, G. L., "The Composition of the Exhaust Products of Military Weapons," Technical Report R-1948, March 1970, Frankford Arsenal, Philadelphia, Penna.

Thermal conductivity, k_g[15] = 2.5×10^{-2} BTU/hr-ft °R

Prandtl number, P_r = 2.905

Recovery factor, RF = 1.43

Propellant gas composition[16]

Compound	Composition in Mole Fraction
H_2	0.1531
H_2O	0.1968
CO	0.4419
N_2	0.1078
CO_2	0.0986

[15] Price, E. W., et al., "Theory of Ignition of Solid Propellants," AIAA Journal, Vol. 4, July 1966.

[16] Stiefel, L., and Hody, G. L., "The Composition of the Exhaust Products of Military Weapons," Technical Report R-1948, March 1970, Frankford Arsenal, Philadelphia, Penna.

APPENDIX B

Determination of Intermediate Mach Number

Bore length, L = 0.062 inch
Bore diameter, D = 0.0135 inch
Friction factor, f = 0.002
Inlet Mach number, M = 0.865

1. The bore length required for the Mach number to change from 0.865 to 0.90.

$$\frac{4fL}{D} = \left(\frac{4fL}{D}\right)_{M_1} - \left(\frac{4fL}{D}\right)_{M_2} = \left(\frac{4fL}{D}\right)_{.865} - \left(\frac{4fL}{D}\right)_{.900}$$

$$= .0367 - .0174 = .0193$$

$$L = \frac{(.0135)(.0193)}{(4)(.002)} = 0.032 \text{ inch}$$

The Mach number increases to 0.90 after 0.032 inch.

2. The bore length required for the Mach number to change from 0.90 to 0.95.

$$\frac{4fL}{D} = \left(\frac{4fL}{D}\right)_{M_1} - \left(\frac{4fL}{D}\right)_{M_2} = \left(\frac{4fL}{D}\right)_{.900} - \left(\frac{4fL}{D}\right)_{.950}$$

$$= .0174 - .00395 = .01345$$

$$L = \frac{(.0135)(.01345)}{(4)(.002)} = 0.0226 \text{ inch}$$

The Mach number increases from 0.865 to 0.95 after 0.032 inch + 0.0226 inch = 0.0546 inch.

3. The bore length required for the Mach number to change from 0.95 to 1.00.

$$\frac{4fL}{D} = \left(\frac{4fL}{D}\right)_{M_1} - \left(\frac{4fL}{D}\right)_{M_2} = \left(\frac{4fL}{D}\right)_{.95} - \left(\frac{4fL}{D}\right)_{1.00}$$

$$= .00395 - 0 = .00395$$

$$L = \frac{(.0135)\ (.00395)}{(4)\ (.002)} = 0.0066 \text{ inch}$$

The Mach number increases from 0.865 to 1.00 after 0.032 inch + 0.0226 inch + 0.0066 inch = 0.0612 inch.

Summary for f = 0.002

z	M
0	0.865
0.032	0.90
0.0546	0.95
0.0612	1.00

APPENDIX C

Calculation of Gas Properties at Intermediate Locations (f=0.002)

Chamber conditions

$T_o = 5040\,°R$

$P_o = 2.5 \times 10^4$ psi

$\rho_o = 11.09\ lb_m/ft^3$

1. z = 0 (inlet conditions)

Isentropic Process

M	= .865	
T_∞	= 4624 °R	(equation (4))
P_∞	= 16025 psi	(equation (5))
ρ_∞	= 7.75 lb_m/ft^3	(equation (6))
v_∞	= 2981 ft/sec	(equation (7))
P_o	= 2.5×10^4 psi	(given)
T_o	= 5040 °R	(given)

2. z = 0.062 (exit conditions)

Adiabatic Process

M	= 1.0	
T_o	= 5040 °R	(given)
T_∞	= 4500 °R	(equation (4), M = 1)
$\frac{P}{P^*}$	= 1.173	
P^*	= $\frac{16025}{1.173}$ = 13661 psi	(gas tables)
ρ_∞	= $\frac{(13661)\,(144)}{(64.372)\,(4500)}$	(equation (3))
ρ_∞	= 6.79 lb_m/ft^3	
P_o	= (1.795) (13661)	(equation (5), M = 1)
P_o	= 24521 psi	
v	= $1\sqrt{(1.24)\,(2072.7)\,(4500)}$	(equation (7), M = 1)
v	= 3400 ft/sec	

3. $z = 0.032$ (intermediate conditions)

Adiabatic Process

$M = 0.90$

$T_o = 5040°R$ (given)

$T_\infty = 4593°R$ (equation (4), M = .90)

$\frac{P}{P^*} = 1.123$

$P = (1.123)(13661)$ (gas tables)

$P_\infty = 15341$ psi

$\rho_\infty = \frac{(15341)(144)}{(64.372)(4593)}$ (equation (3))

$\rho_\infty = 7.47\ lb_m/ft^3$

$v = .90\sqrt{(1.24)(2072.7)(4593)}$ (equation (7), M = .90)

$v = 3092$ ft/sec

$P_o = (13341)(1.61)$ (equation (5), M = .90)

$P_o = 24699$ psi

4. $z = 0.0546$ (intermediate conditions)

Adiabatic Process

$M = 0.95$

$T_o = 5040°R$ (given)

$T_\infty = 4547°R$ (equation (4), M = .95)

$\frac{P}{P^*} = 1.0583$

$P = (1.0583)(13661)$ (gas tables)

$P_\infty = 14458$ psi

$\rho_\infty = \frac{(14458)(144)}{(64.372)(4547)}$ (equation (3))

$\rho_\infty = 7.11\ lb_m/ft^3$

$v = .95\sqrt{(1.24)(2072.7)(4547)}$ (equation (7), M = .95)

$v = 3247$ ft/sec

$P_o = (1.705)(14458)$ (equation (5), M = .95)

$P_o = 24650$ psi

APPENDIX D

Calculation of h_{cz} at z = 0.030 inch

By definition

$$h_{cz} = \frac{Nu_z \, k_g}{z}$$

$$Nu_z = 0.0288 \, (P_r)^{1/3} \, (Re_z)^{4/5}$$

Fluid Properties must be evaluated at

$$T^* = T_\infty + .50 \, (T_o - T_\infty) + .22 \, (T_o - T_\infty)$$

at $z = 0.030$ inch, $T_\infty = 4605°R$, $T_o = 5040°R$

$$T^* = 4605 + .50 \, (5040 - 4605) + .22 \, (5040 - 4605)$$

$$T^* = 4918°R$$

$$\rho_\infty = \frac{P_\infty}{RT^*} = \frac{(15600) \, (144)}{(64.372) \, (4918)} = 7.09 \ lb_m/ft^3$$

$$v_\infty = M\sqrt{\gamma RT^*} = .89\sqrt{(1.24) \, (2072.7) \, (4918)} = 3164 \ ft/sec$$

$$h_{cz} = \frac{(0.0288) \, (1.43) \, (v_\infty \rho_\infty z/\mu)^{4/5} \, k_g}{z}$$

$$h_{cz} = \frac{(0.0288) \, (1.43) \left(\frac{(3164) \, (7.09) \, (0.030)}{(4.72 \times 10^{-5}) \, (12)} \right)^{4/5} (2.5 \times 10^{-2})}{0.030/12}$$

$$h_{cz} = 2.97 \times 10^{-4} \ BTU/ft^2 \, hr \, °R$$

REFERENCES

1. Miller, S., "Design, Development and Fabrication of 100,000 Cartridges, Ball, Caliber .50, M33 Type Assembled with Case, Cartridge Aluminum, Caliber .50, FAT 39," Technical Report R-1265, June 1956, Frankford Arsenal, Philadelphia, Penna.

2. Summerfield, M., "Letter to Reed E. Donnard; Subject: 'Cartridge Burn-Through Problem'," Sept. 1969, Princeton University, Guggenheim Aerospace Propulsion Laboratory, Princeton, N. J.

3. Unpublished data, "The Aluminum Cartridge Case 'Burn-Through' Problem - Characteristics, Isolation, and Means of Elimination," Frankford Arsenal, Philadelphia, Penna.

4. Lyman, T., ed., Metals Handbook, Properties and Selection of Metals, 8th ed., Vol. 1, American Society for Metals, Novelty, Ohio, 1961.

5. Lee, J. F., and Sears, F. W., Thermodynamics, Addison-Wesley, Cambridge, Mass., 1955.

6. Shapiro, A. H., The Dynamics and Thermodynamics of Compressible Fluid Flow, Vol. 1, Ronald Press, New York, 1953.

7. Keenan, J. H., and Kaye, J., Gas Tables, Wiley, New York, 1956.

8. Kreith, F., Principles of Heat Transfer, International Textbook Company, Scranton, Penna., 1963.

9. Rohsenow, W. M., and Choi, H., Heat, Mass, and Momentum Transfer, Prentice-Hall, Englewood Cliffs, N. J., 1961.

10. Olson, R. M., Essentials of Engineering Fluid Mechanics, International Textbook Company, Scranton, Penna., 1962.

11. Ackerman, G., Forsch, Gebiete Ingenieurw, Vol. 13, 1942.

12. Ozisik, M. N., Boundary Value Problems of Heat Conduction, International Textbook Company, Scranton, Penna., 1968.

13. Eckert, E. R. G., Transactions of the American Society of Mechanical Engineers, Vol. 78, 1956.

14. Unpublished data, "Smokeless Powder for Small Arms Ammunition, Nominal Characteristics of Standard Products," Olin Corporation, New Haven, Conn., Oct. 1966

15. Price, E. W., et al., "Theory of Ignition of Solid Propellants," AIAA Journal, Vol. 4, July 1966.

16. Stiefel, L., and Hody, G. L., "The Composition of the Exhaust Products of Military Weapons," Technical Report R-1948, March 1970, Frankford Arsenal, Philadelphia, Penna.